Applying a Numerical Simulation Technique to the Design of WDM-Pumped Raman Amplifiers, and Methods for the Automatic Determination of Pump Powers

*by Koji Fujimura *, Atsushi Oguri *, Takeshi Nakajima *, Yoshihiro Emori *, Shu Namiki * and Misao Sakano **

ABSTRACT In the design of Raman amplifiers, it is necessary, with such characteristics as pump wavelength, pump power, signal power given, to arrive at a numerical prediction of the corresponding output signal power, Raman gain, noise figure, multipath interference, etc. Further, if the values for pump wavelength and pump power that are required to obtain the various target characteristics can be obtained, the efficiency with which the Raman amplifier can be designed is significantly increased. This paper first describes the numerical simulator used to estimate amplifier characteristics. It then proposes a Raman amplifier structure that gradually increases the number of pump wavelengths, and applies the numerical simulator to its design. Finally it discusses a technique for predicting the pump power to be applied in order to obtain the desired values of output signal power and Raman gain.

1. INTRODUCTION

The use, in an optical transmission system using wavelength division multiplexing (WDM), of a distributed WDM-pumped Raman amplifier for optical amplification is effective in reducing noise and broadening gain bandwidth [1), 2)]. We have developed a numerical simulator for the prediction of Raman amplifier characteristics, in a model incorporating the input and output characteristics of the signal, the noise figure, multipath interference (MPI) due to Rayleigh scattering, and nonlinear phase shift. We have also made proposals relating to Raman amplifier structure and pump techniques using this numerical simulator [3), 4)]. Recently we have proposed and designed an amplifier in which the pump wavelength is gradually increased (an upgraded Raman amplifier) using that simulator, and have evaluated its characteristics [5)].

In designing a Raman amplifier, the crucial point is to obtain the pump wavelength and pump power for achieving the various characteristics required. In the simulator described above, the values in the design are selected by human agency, and human decisions and modifications of the design values are reiterated until the characteristics obtained by the simulator satisfy the required characteristics. It is to be hoped that, by further improving the efficiency of the design system, it will be possible to determine automatically the pump wavelength and pump power that satisfy the characteristics. As of the present time a number of techniques have been proposed to determine pump wavelength and pump power by assigning the characteristics to be satisfied in terms of signal output and gain [6)~8)]. Further a superposition rule was developed to determine the pump wavelength for obtaining the target gain characteristics [2)]. We have developed a technique using linear approximation for the automatic determination of pump power [9)]. This is a technique that exhibits a strong convergence to true values even when the initial value departs from the solution.

This paper first describes the numerical simulator used to predict Raman amplifier characteristics, and then, as an example of a design using it, reports on a bandwidth upgradable Raman amplifier. Finally it discusses an automatic design technique for predicting pump power.

2. BASIC EQUATIONS AND DESIGN SUPPORT SYSTEM

2.1 Structure of the Raman Amplifier

Light incident on an optical fiber excites the optical phonons of the glass molecules, loses energy and is scattered as low-frequency light. The phenomenon is known as Raman scattering, and in silicate fibers the frequency shift is normally distributed in the vicinity of 13 THz. If light is present in the scattered light band, stimulated emission occurs, allowing use as a Raman amplifier.

Figure 1 shows the basic structure of a Raman amplifier. It involves an optical signal input of a plurality of wavelengths, pumping lasers having different wavelengths, optical fiber as the gain medium, and a coupler for the signal light and pumping light. In

* Fitel-Photonics Lab., R&D Div.

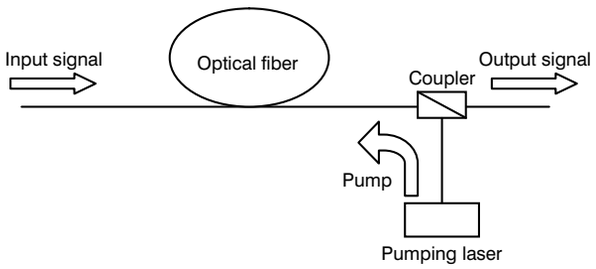

Figure 1 Basic structure of Raman amplifier.

the case of WDM pumping, superposition of the gain characteristics of each pump wavelength makes it possible to achieve the target gain characteristic--e.g. an extremely flat gain characteristic--over a broad bandwidth. Thus in designing a Raman amplifier it is necessary to determine the pump wavelengths and pump powers for obtaining the target characteristic.

2.2 Basic Equations

In WDM transmission, the propagation along the fiber of the time average value of optical power is given by the following differential equation [2), 10), 11)]

$$\pm\frac{dP_\nu^{\pm}}{dz} = -\alpha_\nu P_\nu^{\pm} + \varepsilon_\nu P_\nu^{\mp} + P_\nu^{\pm}\sum_{\mu>\nu} E_{R\mu,\nu}(P_\mu^{+}+P_\mu^{-}) - P_\nu^{\pm}\sum_{\mu<\nu}\frac{\nu}{\mu}E_{R\nu,\mu}(P_\mu^{+}+P_\mu^{-}) + 2h\nu\sum_{\mu>\nu}E_{R\mu,\nu}(P_\mu^{+}+P_\mu^{-})\left[1+\frac{1}{\exp\left[\frac{h(\mu-\nu)}{kT}\right]-1}\right]\Delta\nu \quad (1)$$

where:

P_ν^{+} is the average power of the light (the subscript ν is the frequency of that light and the plus and minus signs indicate propagation in the forward and backward directions respectively),

ε_ν is the backward Rayleigh scattering coefficient of light of frequency ν,

$E_{R\mu,\nu}$ is the nonpolarized Raman gain efficiency from light of frequency μ to light of frequency ν,

$\Delta\nu$ is the infinitesimal bandwidth around frequency ν,

h is Planck's constant,

k is Boltzmann's constant, and

T is absolute temperature.

α_ν is the fiber loss constant at frequency ν and includes the spontaneous Raman scattering effect, and may be represented by

$$\alpha_\nu = \alpha_\nu^{*} + 4h\nu P_\nu^{\pm}\sum_{\mu<\nu}E_{R\nu,\mu}\left[1+\frac{1}{\exp\left[\frac{h(\nu-\mu)}{kT}\right]-1}\right]\Delta\nu \quad (2)$$

where:

α_ν^{*} is the fiber loss constant not including the Raman scattering effect.

So summarizing, from Equation (1), the 1st term represents the effect of fiber loss, the 2nd that of Rayleigh scattering, the 3rd and 4th that of stimulated Raman scattering, and the 5th that of spontaneous Raman scattering.

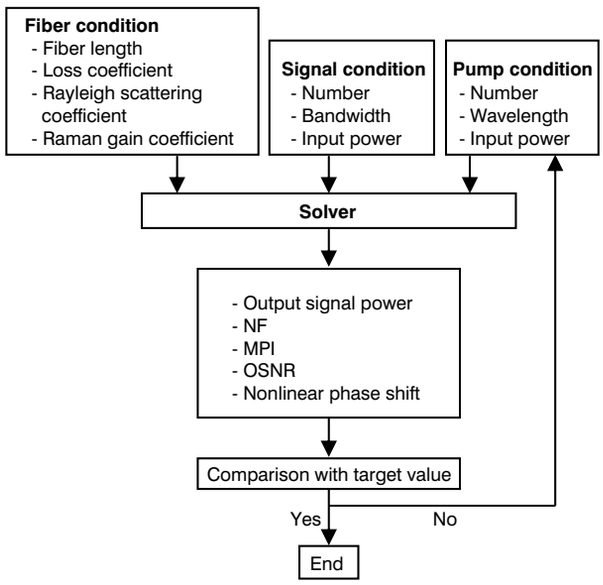

Figure 2 Flowchart of design support system of WDM-pumped Raman amplifier.

2.3 Design Support System

In order to determine the pump wavelengths and pump powers that would give the target gain characteristics, we have configured a design support system that provides numerical solutions to Equations (1) and (2). Since in solving these differential equations we must deal with light propagating in both the forward and backward directions, we have to solve problems having boundary values at two points--the input and output sides. To do this we have used a 4th-order Runge-Kutta method that solves iteratively for the forward and backward directions.

Figure 2 shows a flowchart of the design support system. When the fiber condition, signal condition and pump condition are input to the solver, characteristics of output signal power, noise figure (NF), multipath interference (MPI), optical signal-to-noise ratio (OSNR) and nonlinear phase shift are output. It is then determined whether or not these match the design specifications, and if they are found to match the design is complete. If they do not match, the pump conditions are modified and the process is repeated until they do.

In Figure 3(a) through (f) are shown typical output windows for Raman gain, NF, net gain, MPI, OSNR and nonlinear phase shift.

3. BANDWIDTH-UPGRADABLE RAMAN AMPLIFIERS

3.1 Background and Amplifier Structure

With increases in the traffic volume on optical communication systems, it is anticipated the signal bandwidth used in WDM system will become broader.

Rather than providing bandwidth for future demand from the outset, however, it will be more desirable, from the standpoint of decreasing initial invsetment, to effect bandwidth upgrading as the need arises. Since with Raman amplifiers the amplification bandwidth can be easily increased by WDM-pumping, making it possible to address these needs by adding pump wavelengths.

An example of a Raman amplifier with upgradable amplification bandwidth has already been reported, in which, by adding 3 pump wavelengths, an upgrade was effected in one step from C band or L band to C+L band[2]. To achieve a more flexible response to market demand, however, it would be preferable to upgrade using a narrower amplification width.

Accordingly in this paper we report on a Raman amplifier unit with an amplification bandwidth that is upgradable from approximately 20 nm to 75 nm at 8-nm (1-THz) intervals, as shown in Figure 4, using backward pumping of an 80-km TrueWave® RS nonzero dispersion-shifted fiber. There are two methods of upgrading the amplification bandwidth: a) by adding pump wavelengths toward the shorter wavelengths and b) by adding pump wavelengths toward the longer wavelengths, and we conducted investigations into which of them is most advantageous in terms of pumping light cost.

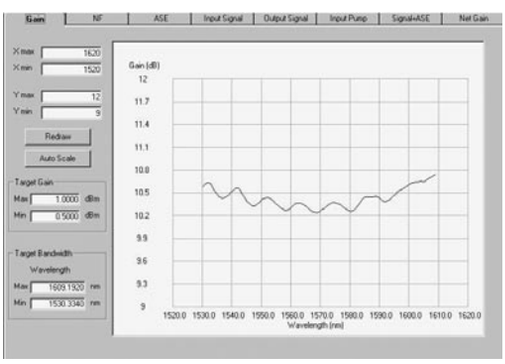

(a) Raman gain

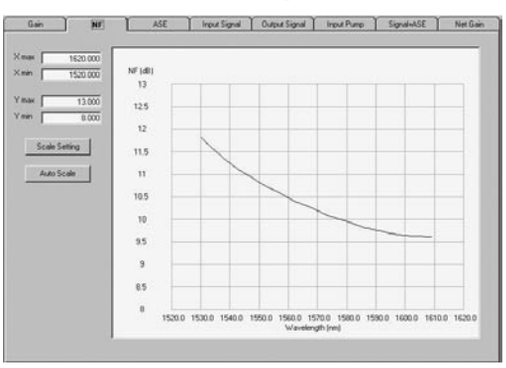

(b) NF

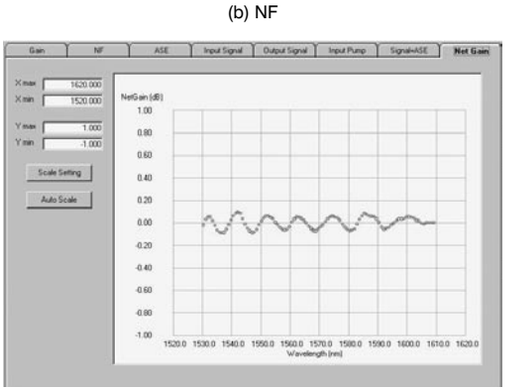

(c) Net gain

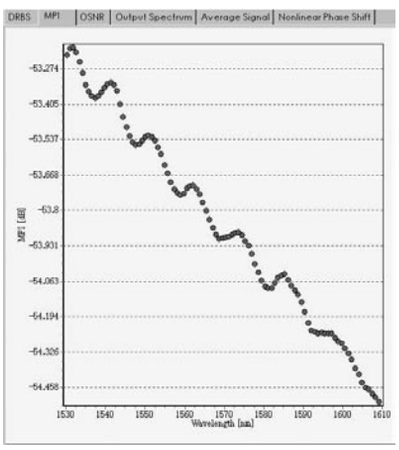

(d) MPI

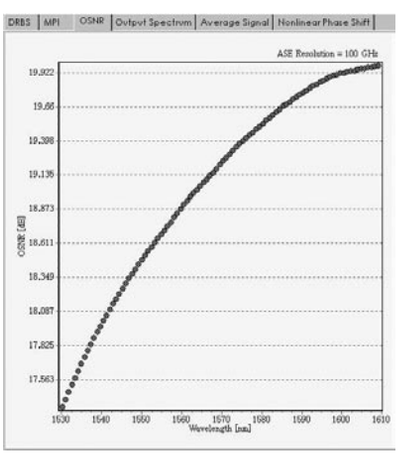

(e) OSNR

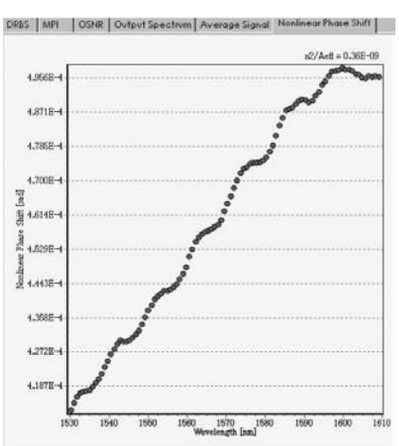

(f) Nonlinear phase shift

Figure 3 Output windows of design support system for WDM-pumped Raman amplifier.

† TrueWave® is a registered trademark of OFS Fitel.

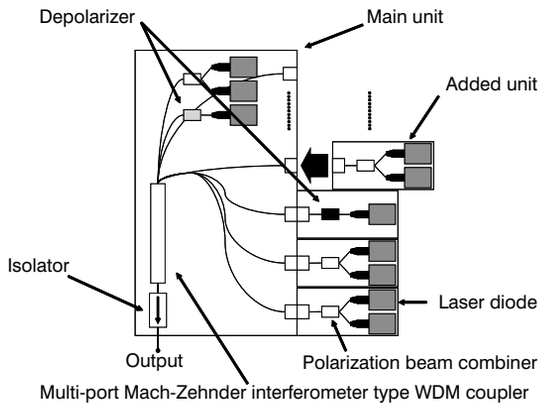

Figure 4 Schematic of bandwidth-upgradeable Raman amplifier.

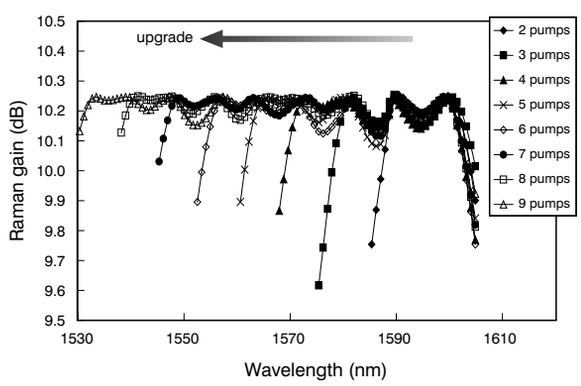

a) When upgraded toward shorter wavelengths

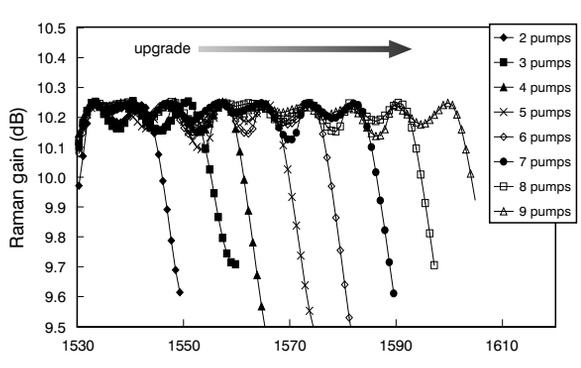

b) When upgraded toward longer wavelengths

Figure 5 Simulated Raman gain profiles.

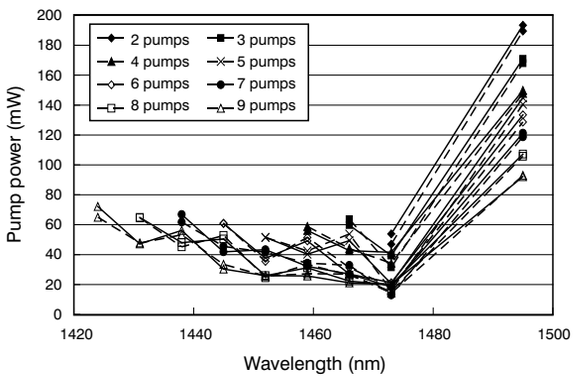

a) When upgraded toward shorter wavelengths
(solid lines show experimental results;
dashed lines show simulation results)

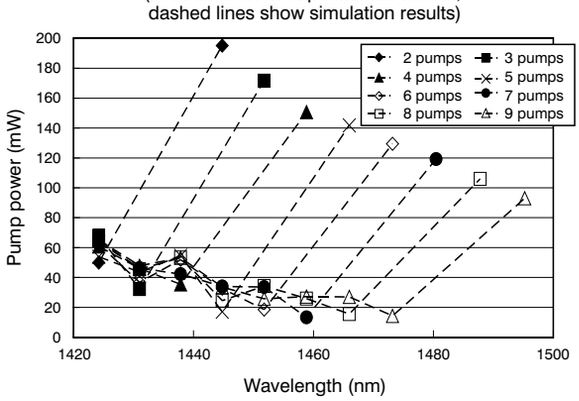

b) When upgraded toward longer wavelengths

Figure 6 Pump power required at each stage of upgrading.

3.2 Simulation Results

Figure 5 shows the results of Raman gain profiles for the two methods of upgrading--toward shorter and toward longer wavelengths. As can be seen both methods have been confirmed to provide adequate flatness of the amplification bandwidth.

Figure 6 shows the results of simulations of pump power when upgraded toward shorter and longer wavelengths. A comparison of the specified pump power required by the two methods of upgrading shown in Figure 6 demonstrates that from the standpoint of the cost of pumping light, the shorter wavelength method of upgrading is superior for two reasons:

The first is that the total of the specified power required at all pump wavelengths was only 662.7 mW when upgraded in the shorter wavelength direction, or about half the 1277.2 mW that was required when upgraded in the longer wavelength direction. This is because when upgraded in the shorter wavelength direction, the pump having the longest wavelength, which required the greatest pump power, was fixed at 1495.2 nm, whereas when upgraded in the longer wavelength direction, it shifted at each stage of the upgrade.

The second reason is that when upgraded in the longer wavelength direction, pump power is required for two extra pumps, at 1480.5 and 1487.8 nm. That is because the longest pump wavelength used is 1480.5 nm for 7 pumps and 1487.8 nm for 8. It is for these reasons that upgrading in the shorter wavelength direction is more cost effective. It can further be seen that when upgraded in the shorter wavelength direction the specified power required for pump wavelengths other than the longest (1495.2 nm) is comparatively small--no more than 80 mW.

3.3 Experimental Results

To verify the results of simulation, experiments were carried out for upgrading in the shorter wavelength direction under conditions similar to those of the simulation. As Figure 7 shows it was possible to obtain Raman gain similar to that in the simulation in Figure 5(a). Figure 6(a) compares the pump power obtained

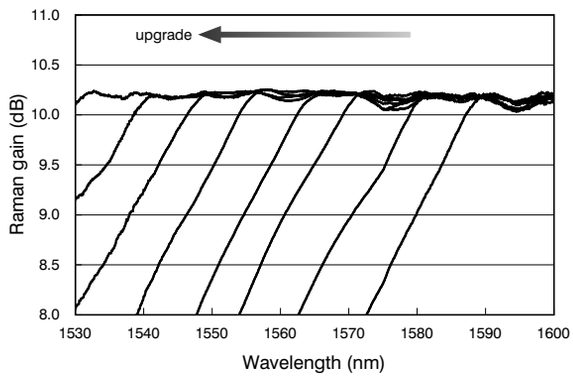

Figure 7 Raman gain profiles from experiments.

experimentally (solid lines) and by simulation (dashed lines), confirming a good agreement between the experimental and simulated values.

4. AUTOMATIC DESIGN AND CONTROL

4.1 Guideline for Automatic Design

As was shown in Figure 2, to obtain the target output signal power and gain profile for a WDM-pumped Raman amplifier it is necessary to determine the wavelength and input power for each pump. It is therefore extremely effective to develop a procedure for automatic determination of the distribution of the pump powers. This automatic determination may be obtained by following the flowchart shown in Figure 8, whereby signal condition and fiber condition are input together with the target value for output signal power, and the optimum pump conditions are determined by solving the inverse problem by numerical calculation.

Methods previously used to solve the inverse problem include a genetic algorithm [6], simulated annealing algorithm [7], and neural networks [8]. In all these methods the optimum settings for pump wavelengths and pump powers are determined simultaneously. And since it is a nonlinear problem there are disadvantages, in that the optimization takes time and a unique solution cannot be obtained. Again, a method that uses a superposition rule to determine the optimal pump wavelengths has also been developed in the past [2), 12)].

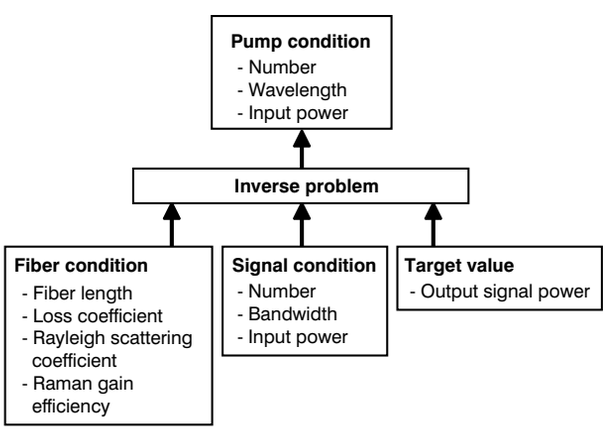

Figure 8 Flowchart for automatic design of WDM-pumped Raman amplifier.

As a guideline for design, we propose a method in which pump powers are optimized after the pump wavelengths have been determined. For determining the optimal pump wavelengths a superposition rule is used. And since the wavelength of the 14xx nm pumping laser is in practice fixed, it is effective to optimize the pump powers setting with respect to the existing pump wavelength settings.

4.2 Algorithm

Following is an explanation of the algorithm for automatic determination of optimal pump powers after determining optimum pump wavelengths. First we ignore the Rayleigh scattering term and spontaneous Raman scattering term in Equation (1), which have virtually no effect on the optimization of pump power. Also, for simplicity we assume a single signal light and a single forward pump. As the initial condition we take the longitudinal distribution of signal power to be $P_{S0}(z)$ and that of pump power to be $P_{P0}(z)$. Further, let the amounts of change in power from the initial to target values be defined as $\varepsilon(z)$ and $\nu(z)$, and let the longitudinal distribution of target signal power and pump power be $P_S(z)$ and $P_P(z)$, respectively. Thus we have:

$$\begin{aligned} P_S(z) &= P_{S0}(z) + \varepsilon(z) \\ P_P(z) &= P_{P0}(z) + \eta(z) \end{aligned} \tag{3}$$

Since $P_{S0}(z)$, $P_{P0}(z)$, $P_S(z)$ and $P_P(z)$ all satisfy Equation (1), they may be substituted, yielding a differential equation relating to ε and ν. Then by ignoring the 2nd-order terms for ε and ν we obtain the linear differential equation

$$\begin{pmatrix} \dfrac{d\varepsilon(z)}{dz} \\ \dfrac{d\eta(z)}{dz} \end{pmatrix} = \begin{pmatrix} -\alpha_S + g_{SP}P_{P0}(z) & -g_{SP}P_{S0}(z) \\ -g_{PS}P_{P0}(z) & -\alpha_P - g_{PS}P_{S0}(z) \end{pmatrix} \begin{pmatrix} \varepsilon(z) \\ \eta(z) \end{pmatrix}$$

$$= \mathbf{F} \begin{pmatrix} \varepsilon(z) \\ \eta(z) \end{pmatrix} \tag{4}$$

where: α_S and α_P are the fiber loss coefficients for the signal light and pumping light respectively, g_{SP} is the Raman gain efficiency between the pumping light and the signal light, and may be expressed as $g_{PS} = (\nu_P/\nu_S)g_{SP}$ (ν_S and ν_P being the frequencies of the signal light and pumping light respectively).

Since the members of matrix $\mathbf{F}$ in Equation (4) are functions of z, it cannot be solved by direct analysis. Thus the fiber is divided into N sectors, with a sector length so minute that $P_{S0}(z)$ and $P_{P0}(z)$ can be considered constant within that sector.

In this way, if differential equation (2) is solved for the sector from $z=z_i$ to $z=z_{i+1}$, we obtain the simultaneous equation

$$\begin{pmatrix} \varepsilon(z_{i+1}) \\ \eta(z_{i+1}) \end{pmatrix} = \mathbf{A}_i \begin{pmatrix} \varepsilon(z_i) \\ \eta(z_i) \end{pmatrix} \quad (5)$$

and if Equation (5) is applied iteratively from $z=0$ to $z=L$, we obtain the simultaneous equation

$$\begin{pmatrix} \varepsilon(L) \\ \eta(L) \end{pmatrix} = \mathbf{A}_N \mathbf{A}_{N-1} \ldots \mathbf{A}_2 \mathbf{A}_1 \begin{pmatrix} \varepsilon(0) \\ \eta(0) \end{pmatrix} = \mathbf{A} \begin{pmatrix} \varepsilon(0) \\ \eta(0) \end{pmatrix} \quad (6)$$

If this is expanded to m signal light of wavelengths and n pumping wavelengths, we obtain the simultaneous equation

$$\begin{pmatrix} \varepsilon_1(L) \\ \vdots \\ \varepsilon_m(L) \\ \eta_1(L) \\ \vdots \\ \eta_n(L) \end{pmatrix} = \mathbf{A} \begin{pmatrix} \varepsilon_1(0) \\ \vdots \\ \varepsilon_m(0) \\ \eta_1(0) \\ \vdots \\ \eta_n(0) \end{pmatrix} \quad (7)$$

Equation (7) represents a relational expression for the input and output sides of the amount of change in signal power and pump power respectively. If the total number of the equations is greater than that of the unknown quantities, those unknown quantities can be found by the linear least squares method.

Up to this point the discussion has concerned the linear domain within which the amount of change is assumed to be minute, but can be extended into a method capable of addressing larger amounts of change. The amount of change is determined not in one step only as the difference between the initial and target values, but within a range in which linear approximation is useful. It is then continued, by iterative steps, until it matches the target value. The usefulness of this method depends on the width of the steps in the change in power. Since it is a linear problem, the calculation can be carried out in a very short time.

If a little more time is expended, a design of extremely high accuracy can be achieved. It is sufficient to apply the design support system once or twice in the final step to reach a direct numerical solution to Equation (1), to revise the longitudinal distribution of signal power and pump power to a precise value. We have called the method in which Equation (1) is solved in the final step the "high-accuracy procedure" and that in which it is not solved in the final step the "high-speed procedure."

4.3 Verifying Accuracy

To verify the accuracy of the design method described above, we derived Raman gain spectra from the pump power allocation optimized using the method and compared them with those obtained by the superposition rule. For the Raman amplifier we used 100 km of dispersion-shifted fiber (DSF), 10 backward pumps, and 97 signal channels from 1530 to 1610 nm at 100-GHz spacing. We assumed an input signal power of 0 dBm/ch and pump wavelengths already given. Pump powers were optimized so that Raman gain of 20 dB was realized throughout the signal bandwidth. The Raman gain spectrum used as the initial value averaged approximately 2 dB, a difference of 18 dB from the target value.

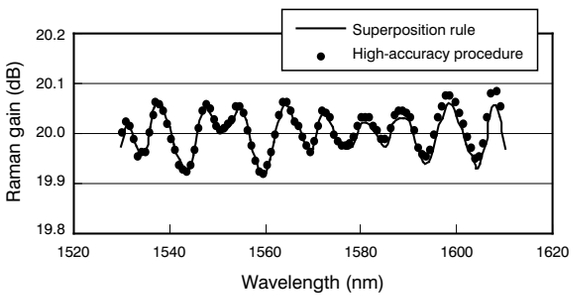

Figure 9 Raman gain spectra.

Figure 9 shows the Raman gain spectra resulting from the design. The results from the high-accuracy procedure are in virtually full agreement with the results from the superposition rule, with a difference of 0.03 dB at the most. From these results it can be seen that our method provides an effective means of determining the optimum pump power distribution with respect to given pump wavelengths.

We then attempted verification using the results obtained from the experiments in Section 3 above. Optimum pump powers were determined taking 42 mW as the initial value of pump power for each pump and the Raman gain spectra obtained in the experiments as the target value. This was then compared with the pump powers used in the experiments.

Figure 10(a) shows the Raman gain obtained experimentally, which becomes the target value, and the initial value of Raman gain. The pump powers optimized by the high-accuracy procedure differed from the experimental values by 2 mW in total, and by a maximum of 6 mW with respect to any one of the pumps. This discrepancy, based on a total pump power of 390 mW, was 0.5% and 1.5% respectively. The Raman gain obtained by the high-accuracy procedure agreed with the experimental results to within 0.2 dB. Figure 10(b) shows the Raman gain spectra obtained by the high-speed procedure using step widths of 0.5, 1 and 2 dB, the Raman gain spectra obtained by the high-accuracy procedure, and the Raman gain spectra from experimental results. It can be seen that the smaller the step width is made the closer the approach to the experimental results and the greater the accuracy. What is more the Raman gain spectra obtained at a 0.5-dB step width is in substantial agreement with the results obtained by the high-accuracy procedure.

4.4 Feedback Control Simulation

Finally let us present an example of feedback control simulation for the high-speed procedure. Since the high-speed procedure uses linear approximation for nonlinear equations, it is useful with respect to control from the standpoint of the calculation time. Let us consider a

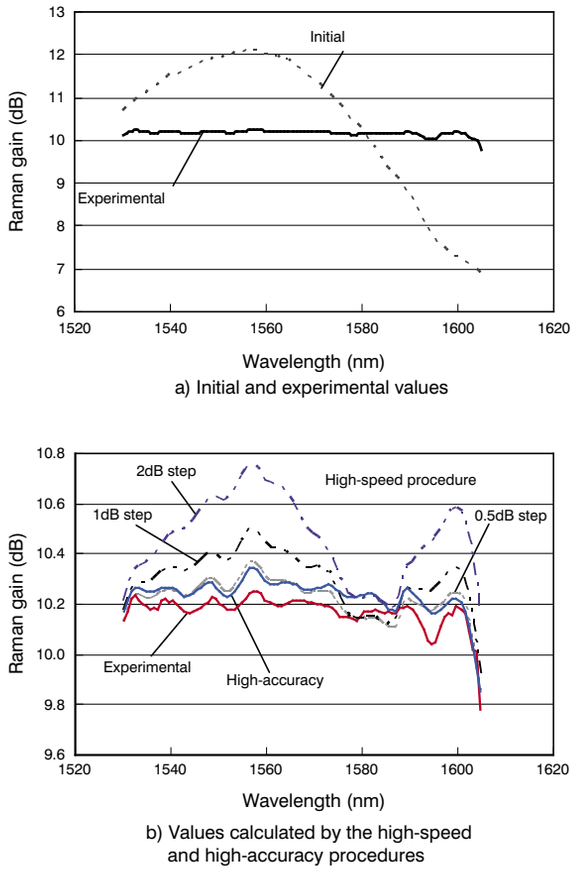

Figure 10 Raman gain spectra.

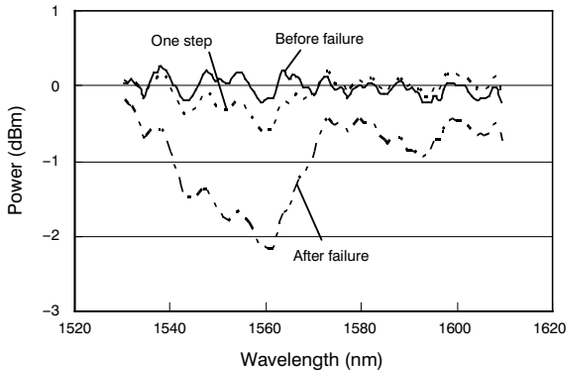

Figure 11 Output signal power before failure, after failure and after control restoration by one step only.

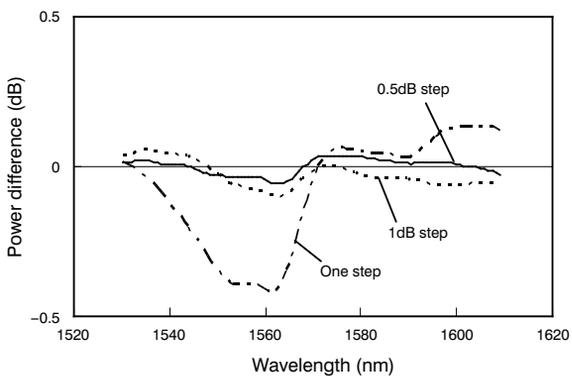

Figure 12 Difference in output signal power from before the failure, obtained by control using a one-step procedure and for step widths of 1 and 0.5 dB.

system in which are connected two Raman amplifiers set to a net gain of 0 dB, each using 100 km of dispersion-shifted fiber (DSF) with 10 backward pumps. The signal condition was 97 signal channels from 1530 to 1610 nm at 100-GHz spacing, and an input signal power of 0 dBm/ch. That is to say the target output signal power was 0 dBm/ch.

Now let us assume a condition in which one of the laser diodes in the first of these Raman amplifiers fails, resulting in the output signal power of the second of the Raman amplifiers deviating from the initial value. To cope with this a process is undertaken whereby the pump powers of the second Raman amplifier are controlled so as to return the output signal power to the initial value. First the output signal power of the second Raman amplifier is monitored, and the amount of change in the signal power input to it is predicted using Equation (7). The distribution of the pump power required to return output signal power to the initial value in then similarly determined using Equation (7).

Figure 11 shows the output signal power before the failure, after the failure and after control restoration based on a procedure of one step only. Control simulations were also carried out for step widths of 0.5 and 1 dB. Figure 12 shows these results in terms of the difference in output signal power from before the failure. As in Figure 10(b), it can be seen that the smaller the step width is made the better the output signal is restored. In the case of a 0.5-dB step width, the flatness (difference between maximum and minimum values) was restored from 1.99 dB to 0.54 dB. This is extremely close to that value of 0.50 dB before the failure.

5. SUMMARY

A numerical simulator has been developed for predicting the characteristics of Raman amplifiers. This simulator has been applied to configuring Raman amplifiers proposed by the authors, having gradually increased numbers of pump wavelengths. Experimental and simulated values were found to be in good agreement, and through comparisons of methods for upgrading in the shorter wavelength direction and the longer wavelength direction, it was found that the shorter wavelength upgrade was desirable in terms of pump light cost.

An automatic design method was also developed for predicting pump powers on the basis of linear approximation. It was confirmed that even when the initial value of pump power diverged from the optimum value (18 dB for Raman gain), this design method showed powerful converging performance.

ACKNOWLEDGMENT

In conducting the research reported here the authors would like to express their thanks to Mr. Akira Aikawa and to Mr. Hiroyuki Katayama of Furukawa Information Technology Corp. for their cooperation in building the simulator.

REFERENCES

1) B. Zhu, L. E. Nelson, S. Stulz, A. H. Gnauck, C. Doerr, J. Leuthold, L. Gruner-Nielsen, M. O. Pedersen, J. Kim, R. Lingle. Jr., Y. Emori, Y. Ohki, N. Tsukiji, A. Oguri, S. Namiki: "6.4-Tb/s (160×42.7 Gb/s) transmission with 0.8 bit/s/Hz spectral efficiency over 32×100 km of fiber using CSRZ-DPSK format," OFC 2003, PD19 (2003).
2) S. Namiki, Y. Emori: "Ultrabroad-band Raman amplifiers pumped and gain-equalized by wavelength-division-multiplexed high-power laser diode," J. of Selected Topics in J. Quantum Electron., vol. 7, no. 1, pp. 3-16 (2001).
3) S. Kado, Y. Emori, S. Namiki: "Gain and noise tilt control in multi-wavelength bi-directionally pumped Raman amplifier," OFC2002, TuJ4 (2002).
4) Y. Emori, S. Matsushita, S. Namiki: "1-THz-spaced multi-wavelength pumping for broadband Raman amplifiers," ECOC2000, vol. 2, pp. 73-74 (2000).
5) A. Oguri, Y. Emori, S. Namiki: "1 THz-step bandwidth upgrades in broadband Raman amplifier by adding pump laser diodes," OFC2003, ThB1 (2003).
6) V. E. Perlin, H. G. Winful: "Efficient design method for multi-pump flat-gain fiber Raman amplifiers," OFC2002, TuJ1 (2002).
7) M. Yan, J. Chen, W. Jiang, J. Li, J. Chen, X. Li: "Automatic design scheme for optical-fiber Raman amplifiers backward-pumped with multiple laser diode pumps," Photon. Tech. Lett., vol. 13, pp. 948-950 (2001).
8) P. Xiao, Q. Zeng, J. Huang, J. Liu: "A new optimal algorithm for multipump sources of distributed fiber Raman amplifier," Photon. Tech. Lett., vol. 15, pp. 206-208 (2003).
9) K. Fujimura, M. Sakano, T. Nakajima, S. Namiki: "A linearized method for unique determination of the input pump powers in designing and controlling WDM-pumped Raman amplifiers," OAA2003, MC3, pp. 56-58 (2003).
10) H. Kidorf, K. Rottwitt, M. Nissov, M. Ma, E. Rabarijaona: "Pump interactions in a 100-nm bandwidth Raman amplifier," Photon. Tech. Lett., vol. 11, pp. 530-532 (1999).
11) M. Ikeda, M. Sakano, H. Katayama, S. Namiki, Y. Emori, S. Kado: "Wavelength Dependence of Raman Gain Efficiency," OECC2002, 10D2-5 (2002).
12) Y. Emori: "Ultra-broadband Fiber Raman amplifiers," ECOC2002, Symposium 3.2 (2002).